Toward a Conceptual Design for MAVIS

Francois Rigaut[a], David Brodrick[a], Guido Agapito[b], Valentina Viotto[c], Cedric Plantet[b], Bernardo Salasnich[c], Richard Mcdermid[d], Giovanni Cresci[b], Simon Ellis[d], Matteo Aliverti[e], Simone Antoniucci[f], Andrea Balestra[c], Andrea Baruffolo[c], Maria Bergomi[c], Marco Bonaglia[b], Giuseppe Bono[f], Lorenzo Busoni[b], Elena Carolo[c], Simonetta Chinellato[c], Gayandhi De Silva[d], Simone Esposito[b], Daniela Fantinel[c], Jacopo Farinato[c], Thierry Fusco[h], Dionne Haynes[a], Anthony Horton[d], Gaston Gausachs[a], James Gilbert[a], Damien Gratadour[a], Davide Greggio[c], Marco Gullieuszik[c], Pierre Haguenauer[i], Visa Korkiakoski[a], Demetrio Magrin[c], Laura Magrini[b], Luca Marafatto[c], Helen Mcgregor[d], Trevor Mendel[a], Stephanie Monty[a], Benoit Neichel[h], Fernando Pedichini[g], Enrico Pinna[b], Elisa Portaluri[c], Kalyan Radhakrishnan[c], Roberto Ragazzoni[c], David Robertson[d], Christian Schwab[d], Rob Sharp[a], Marco Stangalini[f], Stefan Stroebele[i], Elliott Thorn[a], Annino Vaccarella[a], Daniele Vassallo[c], Sudharshan Venkatesan[d], Lew Waller[d], Stacy Warner[a], Frederic Zamkotsian[h], and Hao Zhang1[a]

[a]AAO-Stromlo, Australian National University, Cotter Road, Weston, ACT2600, Australia
[b]INAF - Osservatorio Astrofisico di Arcetri, Largo Enrico Fermi 5, 50125 Firenze, Italy
[c]INAF - Osservatorio Astronomico di Padova, Vicolo dell'Osservatorio 5, 35122 Padova, Italy
[d]AAO-MQ, Macquarie University, 105 Delhi Rd, North Ryde NSW 2113, Australia
[e]INAF - Osservatorio Astronomico di Brera, Via E. Bianchi 46, 23807 Merate, Italy
[f]INAF - Osservatorio Astronomico di Roma, Via E. Bianchi 46, 23807 Merate, Italy
[g]INAF - Direzione Scientifica, Viale del Parco Mellini 84, 00136 Roma, Italy
[h]Laboratoire d'Astrophysique de Marseille, 38 rue Fréd. Joliot-Curie, 13388 Marseille, France
[i]European Southern Observatory, Karl Schwarschild Str. 2, Garching b. Munchen, Germany

ABSTRACT

MAVIS, the Multi-conjugate Adaptive-optics Visible Imager-Spectrograph is an instrument being built for the Very Large Telescope Adaptive Optics Facility. The exquisite angular resolution provided by the AO module -in combination with the AOF- will be exploited by a 4kx4k imager and a monolithic IFU covering the optical region. MAVIS is currently in phase A (conceptual design), and the consortium just passed the phase A mid-term review. In this paper, we introduce the project, detail trade-off studies and provide a snapshot of the numerical simulations and current design choices. MAVIS is shaping up to be a truely amazing facility, providing $3\times$ the HST angular resolution with better sensitivity on point sources. MAVIS will be a workhorse facility instrument for the VLT into the 2030s, complementing very effectively facilities like the ELTs, and facing little competition in the current astronomical instrumentation landscape.

Keywords: Astronomical instrumentation, Adaptive Optics, Multi-Conjugate Adaptive Optics, Integral Field Spectrographs, High Angular Resolution

1. INTRODUCTION

The Multi-conjugate Adaptive-optics Visible Imager-Spectrograph (MAVIS), to operate at the Very Large Telescope (VLT) Adaptive Optics Facility (AOF) will be a general-purpose instrument for exploiting the highest possible angular resolution of any single optical telescope available in the next decade, either on Earth or in space, and with sensitivity comparable to or better than larger aperture facilities. The exquisite angular resolution provided by the AO module -in combination with the AOF- will be exploited by a 4kx4k imager and a

---

Send correspondence to `francois.rigaut@anu.edu.au`.

monolithic Integral Field Unit (IFU) covering the optical region. By probing the frontier of angular resolution and sensitivity across a large portion of the observable sky, MAVIS will enable progress on an array of scientific topics, from our own planetary system to those around other stars, and from the physics of star formation in the Milky Way to the first star clusters in the Universe. After an extensive community consultation for future VLT instrumentation, ESO released in May 2018 a call for proposal for VAOI, a Visible AO Imager (and spectrograph). A consortium quickly formed to answer this call for proposal, with the following institutes:

- Australian Astronomical Optics (AAO), specifically the AAO-Stromlo (ANU), lead partner/institute, and AAO-MQ (Macquarie University), Australia; Note that Australia is an ESO strategic partner since July 2017 and for a period of 10 years. This partnership gives Australia access to the LSP observatories, including access to instrument building.

- Istituto Nazionale di Astrofisica (INAF), specifically Arcetri, Padova, Roma and Milano, Italy;

- Laboratoire d'Astrophysique de Marseille(LAM), France;

- European Southern Observatory (ESO), Germany.

The proposal was successful, and the Kick off meeting was held at ESO's headquarters in Garching on Jan31/Feb01 2019.

One particularity of the MAVIS consortium is its geographical scattering. Time difference is 8 to 10 hours and comes with its own challenges. To mitigate this issue, the consortium has adopted a number of measures, that, after 8 months of use, turned out to be fairly efficient. These include regular videocons (we are using zoom), transversal communication (no need to go back through managers for engineers to engineers discussions) and wide adoption of (a) google docs for versioned, collaborative editing and (b) planio[*] for issue tracking/wiki/blog. We also have face to face meetings, e.g. the Kick off meeting and a "busy week" held in Asiago from 6 to 10 May 2019[†], meeting which was crucial in progressing on alternative project baselines, understanding the TLRs and starting to flow down to subsystem requirements, analysing the science white papers and deriving system requirements, starting to work on interfaces, without mentioning team bonding, although the latter is certainly not the least important.

Science was initially discussed in a pre-proposal workshop held at the AAO-MQ in Sydney in March 2018. As we are writing this paper, approximately 40 scientists from inside and outside the consortium are travelling to Firenze, where a "Science with MAVIS" workshop will take place from November 4 to 8, 2019[‡].

The process we are following during phase A maps into the following schedule: The first part of phase A, through the mid-term review (24-25 Oct 2019), was dedicated to:

- Setting up consortium and governance;

- Defining and addressing the most important trade-offs;

- System modelling and performance estimations through numerical simulations;

- Converging toward a baseline design.

The second part of phase A, from the mid term through the final review, will include:

- Synchronising all disciplines with the baseline design (simulations, optical and mechanical designs, etc);

- Going to the next level of details to demonstrate feasibility;

- Generating the phase A review documentation.

---

[*] https://plan.io/
[†] http://mavis-ao.org/mavis/2019/05/23/asiago-busy-week.html
[‡] https://indico.ict.inaf.it/event/850/

The phase B, if approved, will start early 2021. The first light is envisaged for the end of 2026, in line with the current schedule for the european Extremely Large Telescope (ELT); a powerful driver for MAVIS in the visible being the synergy with MICADO in the NIR (and to a lesser extent, HARMONI), both reaching a similar angular resolution over a similar field of view, providing extremely useful additional wavelength range which will enhance greatly sensitivity in many astrophysical programs (see science section).

1.1 Science and Top Level Requirements

ESO's conception of MAVIS is one of a facility instrument. The MAVIS consortium started very early to get the community on board to probe and establish what science programs be enabled by such a facility - or would benefit from it. This led to an initial workshop in Sydney in March 2018, followed by a call for white papers, led by the project scientists, Richard McDermid and Giovanni Cresci.
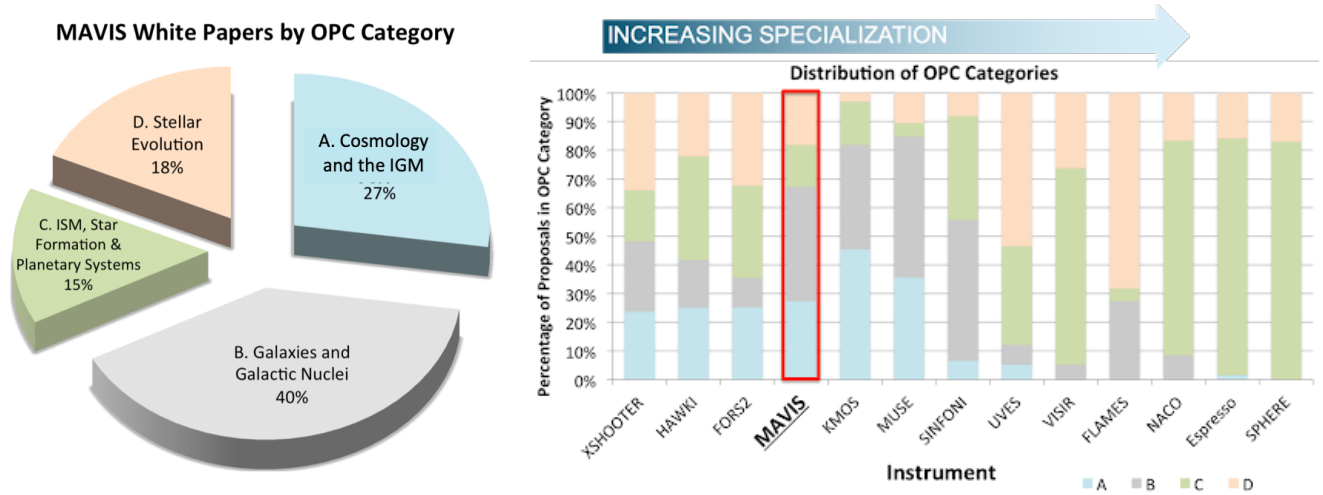

Figure 1. Left: MAVIS white papers distributed along ESO OPC categories. Right: Same analysis for all VLT instruments, in which the instruments are ranked by increased specialisation (i.e. larger imbalance between categories). Based on its preliminary science cases, MAVIS is shaping up to be a general workhorse facility instrument.

Over 57 white papers were received, totalling 270 pages, from 150 scientists (47 institutions). The white papers are available at http://mavis-ao.org/whitepapers/. Figure 1 (left) shows the distribution of these white papers along the ESO OPC science categories. On the right are shown the same distribution for various VLT instruments, sorted using a criteria that traces the equipartition along the different OPC categories. We used that as a proxy for "facility" instruments: the more equally distributed, the more "facility" an instrument is; opposite, niche instruments like SPHERE are essentially all within one OPC category (in that case planets).

The Top Level Requirements (TLRs) for MAVIS, stated by ESO in the VAOI call for proposal, are very ambitious. In term of AO performance, they call for 10% V band (goal 15%) Strehl ratio under 0.83" seeing conditions. A simple analysis lead to the conclusion that this results in a very tight error budget, with very little contingency. MAVIS is based on -and kept affordable by- the existing AOF, which is a major cost saver, but also bring its own constraints, in particular meaning MAVIS has to use the existing DSM (which sets the fitting error), and the existing Laser Guide Star Facility (LGSF), both being excellent but necessarily reducing the degrees of freedom when designing the instrument to match the requirements.

As will be shown in section 3, this tight performance requirements quickly led to the conclusion that we had to use 8 (or 6) Laser Guide Stars (LGSs), to keep the tomographic error within bound and 2 post-focal Deformable Mirrors (DMs) for the generalised fitting. We are adopting a no-compromise approach on a number of aspects:

- Near Infrared diffraction limited Tip-Tilt Wavefront Sensors (WFSs) based on SAPHIRA arrays [1], 60" radius technical field;

- High order post-focal DMs (conjugated at 6 and 15km, with pitches of 24 and 36cm); and

- OCAM2K-based LGS WFSs

The MAVIS design and general concept is largely making use of the experience acquired by the team on other relevant instruments like GeMS, ERIS, Sphere and the AOF: lessons learned on Non-Common Path Aberrations (NCPAs), astrometric distortions, calibrations, data reduction, PSF reconstruction, operation, etc.

Note that we consider that the post-Focal instrumentation, even though large in its scope and requiring attention and focus, does not come with major risks. Its cost is an issue though.

2. SYSTEM ANALYSIS AND BASELINE DESIGN SYNTHESIS

The synthesis of the baseline design has been driven by the instrument TLRs and has been informed by rigorous analysis of alternatives and numerical simulation.

2.1 Trade-Offs Studies

The system analysis process employed "trade-off studies" to objectively assess the relative merits where there were alternate options for an architectural or design solution. The project adopted a standard procedure for performing trade-off studies. The standard process ensures clarity, traceability and objectivity, through identifying:

- Identify alternatives (descriptions of possible approaches, literature, etc);

- Identify criteria (questions to be answered, main drivers, go/no-go);

- Evaluation of alternatives (summarised in table, including assigning a weighting to criteria); and

- Recommendation of the preferred alternative.

The following list gives an overview of some of the most significant Phase A trade-off studies.

- **Derotation Scheme**: Alternative options for derotating the science field and LGS constellation were assessed. This decision had major implications for the instrument such as the physical dimensioning of the Adaptive Optics Module (AOM), including which elements must be located within the Nasmyth interface flange, the location, number and type of optical and mechanical rotation elements, etc. The outcome of this study is detailed below.

- **Post-Focal Deformable Mirror Configuration**: This study was to determine the number of post-focal DMs and their characteristics, given various constraints such as performance, cost and complexity. These parameters have implications for the AOM opto-mechanical configuration in addition to affecting the overall performance. The recommendation was to down-scale the AOM optics from the prior size, and to use two 1.5mm pitch DMs with 48x48 actuators.

- **Short Wavelength Performance and Cut-Off**: The blue wavelength cut-off refers to the shortest wavelength at which MAVIS can deliver useful science. This trade-off has many facets and involves iteration with other instrument constraints, as glass selection etc. affects performance across the entire wavelength range. The final performance and optimisation at the blue end is still being analysed.

- **Performance Effects of Dual AO**: The dual AO architecture as originally proposed (using LGS tomographic data to operate DMs for the Natural Guide Star (NGS) WFSs) had implications for the performance, sky coverage and the cost and complexity of the instrument. Analysis was able to demonstrate that some of the benefit of dual AO could instead be realised by using the outer actuators on the post-focal DMs to correct the outer technical field while reducing the instrument cost and complexity by avoiding the additional DMs required for the original dual AO concept.

- **AOM Optical Design**: Three principle AOM design alternatives were considered: a refractive design; a reflective design; and a catadioptric design. The optical design choice had major implications for the instrument and was likewise constrained by other decisions such as the derotation scheme, blue cut-off, etc. The outcome of the study was that both the refractive and reflective designs were feasible but that image quality was superior with the refractive design, which has been selected. More details are provided below.

- **Laser Guide Star Configuration**: This trade-off involved a large body of analyses to simulate and quantify the consequences on AO performance for alternative number of LGSs, LGS asterism and geometry, etc. The outcome was to use a fixed asterism at 17.5" with at least six, and preferably eight, LGSs.

- **Laser Guide Star Detector**: A number of candidate detectors are commercially available, differentiated by cost and performance. These require thorough evaluation as the detector choice has ramifications for the AO performance, mechanical design and overall instrument budget.

- **Spectrograph Modes**: This study evaluated the performance of different spectrograph alternatives against the science objectives and technical considerations. A single monolithic IFU is the best match to the MAVIS science use-cases.

- **Spectrograph Detector**: This considered the performance and other technical factors of various detectors in the context of using them on the MAVIS spectrograph.

- **Imager Design**: This trade-off was to determine the better alternative between selecting an imager with a re-imager, or not.

3. NUMERICAL SIMULATIONS

During the trade-off phase, we ran numerical simulations to assess the sensitivity of the AOM to several design parameters (DM pitch, conjugation altitude, LGS asterism, LGS flux, technical FoV, NGS asterism, etc). Here, we report on the performance obtained for the baseline configuration (see section 4).

We divided the AOM error sources in two sets: the High Order (HO) and the Low Order (LO). Performance are coming from end-to-end simulations using PASSATA [2] (AO-only error terms) for a "good" NGS asterism is reported in Figure 2.
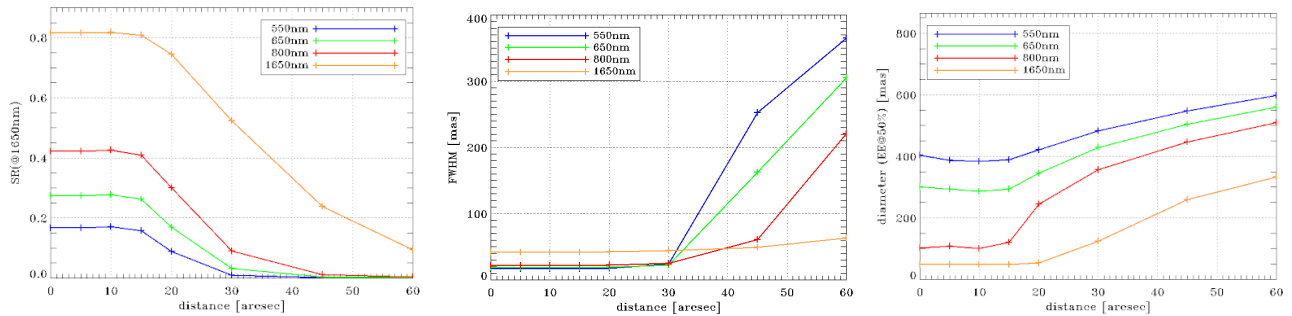

Figure 2. Performance expressed as Strehl ratio (SR), Full-Width at Half Maximum (FWHM) and diameter for 50% of EE, of MAVIS AOM (AO errors only) for a good NGS asterism (bright and near the science field, 20" off-centre).

3.1 High Order

By "high order", we mean all the modes except tip/tilt and quadratic plate-scale modes. HO modes are controlled by LGS WFS measurements and they are separated from low order because of the LGS tip/tilt indetermination problem. The error terms associated with HO are:

- **High Frequencies fitting error**: this error is due the uncorrected spatial frequencies beyond the Nyquist sampling of the corrector (DM) with the smaller pitch (typically, and also for MAVIS, the ground layer DM). In a Single-Conjugate AO (SCAO) system it is the only fitting error term. It decreases with the number of actuators of the DMs.

- **Generalized fitting error**: this error results from the discrete number of correctors. The phase perturbations are spread across the first 15-20km of atmosphere and only a limited number of DMs must correct them. This can be done effectively only if the DMs are conjugated at the same altitude or "near" the phase perturbations. The generalized fitting error decreases with the number of DMs and of actuators of the DMs.

- **Tomographic error**: this error is related to the sensing and reconstruction of the atmospheric turbulence volume. It decreases with the number of guide stars.

- **Aliasing error**: this is related to the maximum spatial frequency that the WFSs can sense. It decreases with the number of sub-apertures of the WFSs.

- **Measurement noise error**: this is related to the signal-to-noise ratio of the measurement. It decreases with the ratio flux - number of controlled actuators/modes.

- **Temporal error**: this is related to the rapid evolution of the turbulence and the delay of the correction.

The values associated with each error term are reported in Table 1, for the baseline design and ESO-specified turbulence conditions (0.83" seeing, Paranal canonical Cn2 profile, etc).

Table 1. Breakdown of AO WFE error terms.

Error Term	Error (nm)
High-frequency fitting error	65.3
Generalized fitting error	33.4
Tomographic error	47.2
Measurement noise error	36.1
Temporal error	34.8
Aliasing error	40.1

3.2 Low orders

By "low order", we mean the tip/tilt, or jitter, in any direction in the FoV, which thus include tip-tilt and plate scale modes. The residual jitter depends on the NGS asterism we have for a given observation. While the HO residuals can be assessed independently from the observed FoV, the jitter residual has to be computed statistically, assuming a certain distribution of the stars. This distribution is taken from the Besancon galaxy model. In the case of MAVIS AOM, the asterisms can have 1, 2 or 3 NGSs depending on the available stars. The statistics of the available stars in the technical FoV is plotted in Figure 3.

The resulting jitter from a given asterism is computed from 3 terms: tomographic error, windshake/temporal error and noise error. The jitter from tomographic error for 1 NGS only is given in figure 4. For 2 NGS, we assume a reduction factor of 1.5 (it varies between 1 and 2 depending on the angle between the NGSs). For 3 NGS, we assume a reduction factor of approximately 3 (it also varies depending on the constellation).

The windshake was arbitrarily scaled from the ELT. It may be pessimistic. The residual jitter as a function of the sensor frame rate is plotted in figure 4 The frame rate is optimized as a trade-off between windshake and noise.
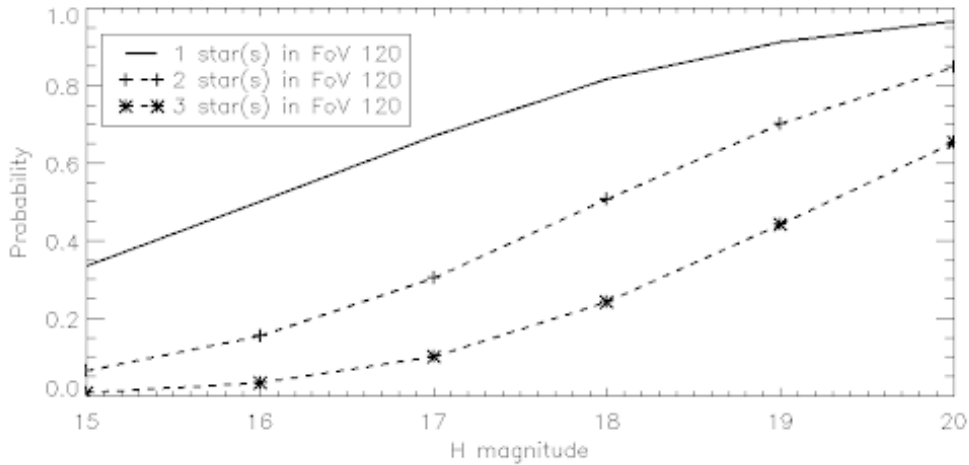
Figure 3. Probability of finding 1, 2 or 3 stars in the technical FoV when pointing towards the South Galactic Pole.

The noise on the tip/tilt measurements is computed with the analytical formulas of the Weighted Center of Gravity from [3], that have been adapted to Strehl ratios less than 1 (by simply scaling the flux by the Strehl ratio). Figure 4 shows the noise jitter for a 50% SR (it is scaled linearly for other SRs). We assume that the noise level on the detector is RON + background = 1 e-.
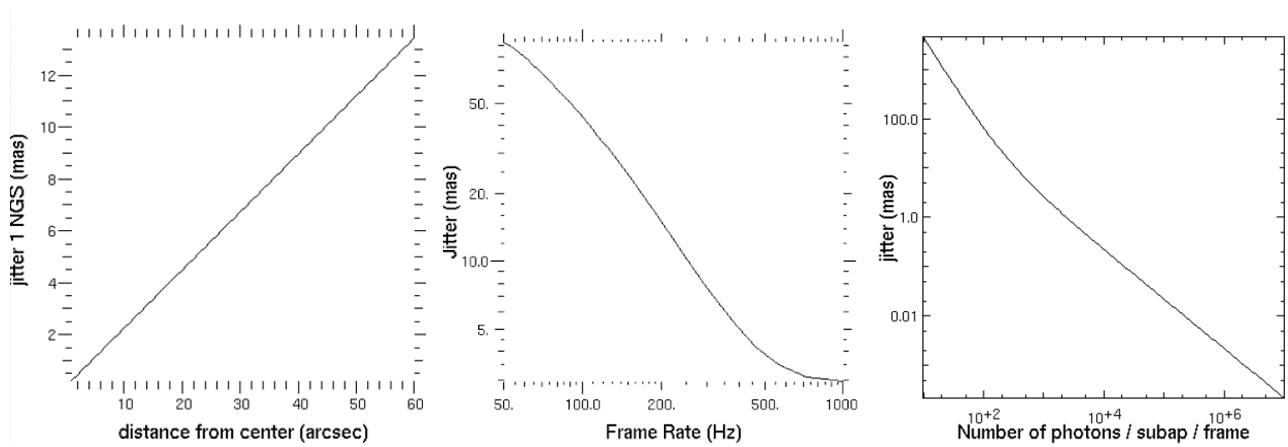

Figure 4. Jitter from tomographic (left), temporal/windshake (middle) or noise (right) error. The tomographic error is given for 1 NGS only.

We applied the computation of the error terms described above to asterisms for a series of random fields. The jitter as a function of the average distance of the NGSs and their total magnitude, as well as the corresponding sky coverage, is plotted in figure 5, assuming the SR variation in the technical Feld of View (FoV) shown in the same figure. We can expect a residual jitter between 10 and 15 mas at 50% sky coverage.

3.3 De-rotation scheme

The way derotation is handled is decisive for the choice of optical design and control strategies, and therefore was one of the choices that came first. To be traded-off were the science and NGS WFS rotation, as well as the LGS constellation rotation and the near field (DSM and post-focal DMs) rotation with respect to the LGS WFSs assembly. Other considerations included the effects on NCPAs, the consequence on the number of optics
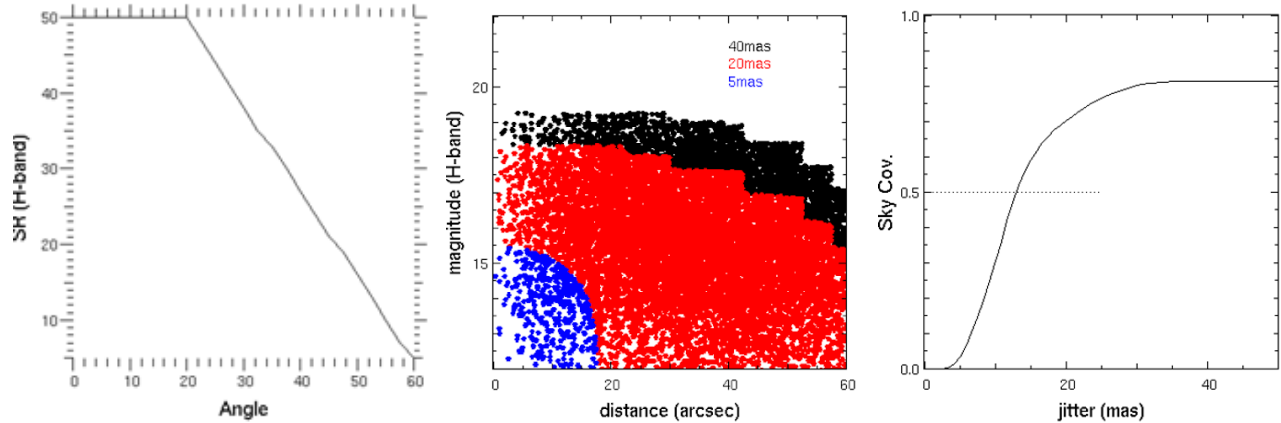
Figure 5. Figure 5. Left: Assumed SR in H band in function of off-axis angle. Middle: Jitter as a function of the average distance of the NGSs and their total magnitude. Right: Sky coverage jitter curve.

and mechanisms, and the flexures. The criteria included performance; cost; impact on the AOF, modularity, testability; simplicity, as opposed to complexity; calibration requirements; feasibility/ease of implementation; robustness and reliability; and availability. Two schemes considered viables, with one coming slightly on top.

In the preferred scheme, the science/common path is derotated at the very entrance of the MAVIS optical bench (see also figure 8 in section 4). Because in this scheme the LGS are fixed with respect to the telescope pupil, they have to be de-rotated within the LGS WFS. This has the beneficial side effect to also derotate the DSM with respect to the LGS WFS, improving the control stability of the latter (mostly by avoiding numerical derotation of the control matrix).

4. BASELINE DESIGN

Figure 6 and Figure 7 provide, respectively, a schematic illustration of MAVIS and the volume allocations for the different modules and sub-modules. The MAVIS design is detailed below, where we describe the main elements, proceeding along the light path.

The AOM Post-Focal Relay (PFR) sub-module presents a refractive optical layout (more details on the trade-off are reported in Greggio et al, this conference), also reported in Figure 8, and includes the elements on the main optical bench from the entrance shutter to the science output port selector. Note this excludes the NGS and LGS WFS sub-modules. The light coming from the telescope enters the system through a shutter located at the Nasmyth focal plane. A Calibration Unit (CU) selection mirror can be used to inject the CU output into the optical train after the shutter, to provide calibration sources for AOM calibration, imaging (flat field, astrometric target) and spectrograph (lines) calibration devices. The foreseen configuration allows to provide means for calibration during daytime, so to minimize the operational overheads during "shutter open" time.

To compensate for the atmospheric dispersion, an Atmospheric Dispersion Corrector (ADC) is located in the PFR common path, followed by a K-mirror, which counter-rotates with the telescope to compensate for the rotation of the field of view, producing a field-stabilised image onto the science and NGS WFS focal planes.

Two post focal Deformable Mirrors (DMs) are set in the optical path to compensate, together with the UT4 Deformable Secondary Mirror (DSM), the effects of the atmospheric turbulence in MCAO mode. In the current MAVIS baseline, the post focal DMs are conjugated at 6 and 15 km from the telescope entrance pupil and are assumed to have a pitch of about 24 and 36 cm on the meta-pupils. All DMs are controlled by the Real Time Controller (RTC), which is part of the AOM, and which controls the DSM through dedicated high-speed interfaces to the UT4 AOF.

The PFR optical train is then separated by a dichroic which allows the NIR light to proceed toward the NGS WFS sub-module. The NGS WFS sub-module is composed of three identical elements which use a pick-up
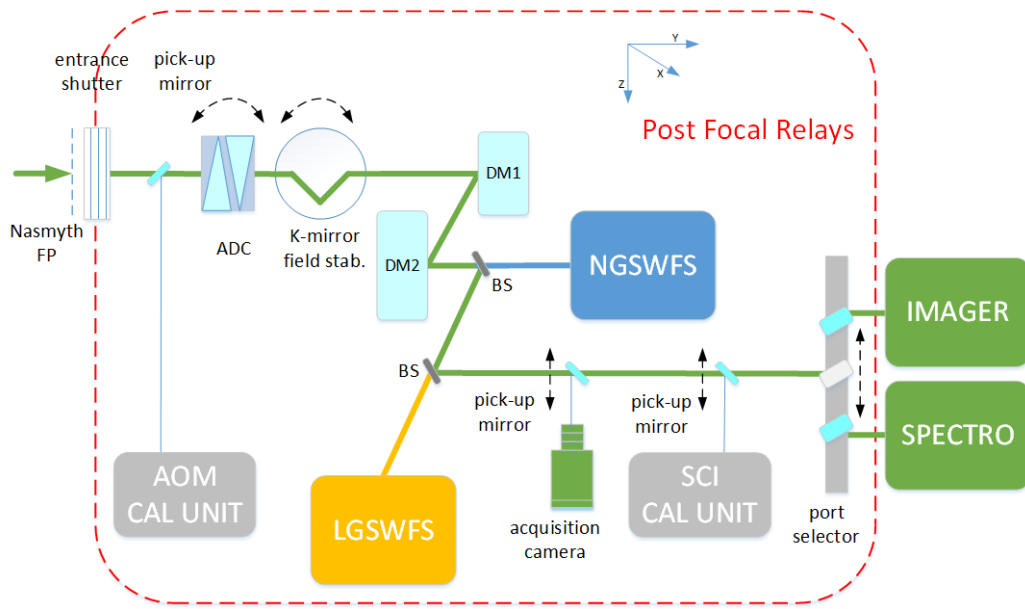
Figure 6. An illustration of the MAVIS conceptual design, showing the AOM Post Focal Relays, NGS WFS and LGS WFS sub-modules, and the Imager, Spectrograph and Calibration Unit modules.

mirror/probe and an XY linear translation stage to select a NGS from the Technical Field of View (TFoV). The probes are located at different levels in the Z axis to avoid collision and have accessibility to the full 2 arcminute diameter TFoV. Each NGS probe directly focuses a F/30 beam onto the corresponding detector, limiting the sensing to tip-tilt mode. The NGS WFS Detector dewar includes also a baffling system for straylight rejection, a blocking filter to get rid of the thermal emission wavelengths longer than H, and a splitting device, which allows to produce two additional images of the NGS onto the same Saphira detector, as depicted in Figure 9, to be used as a truth sensor, using phase diversity (a similar method was used in GeMS for the NCPA control). Non-destructive readout of the detector is assumed, so to allow the TT signal to be retrieved with a much higher framerate (typically 1kHz) than the phase diversity images (typically 0.1 to 1Hz). Both real-time TT signals and slow rate phase diversity images are then treated with a tomographic approach to retrieve the wavefront information in the 30" science FoV.

A second dichroic, with a narrowband response near the 589nm sodium line, is used to feed the Laser Guide Star Wavefront Sensor (LGS WFS) sub-module. The LGS WFS sub-module is composed of an assembly of eight WFSs (one for each LGS), each of which allows a 40×40 pupil sampling, obtained with a Shack-Hartmann array. An optical focusing mechanism allows the sub-module to compensate for the effective height of the sodium layer, changing as a function of the telescope elevation. An additional K-mirror provides means for compensating the differential rotation of the laser asterism with respect to the science FoV, which has been stabilized upstream, in the PFR common path. The overall de-rotation scheme is such that the RTC shall take into account differential rotation between the post focal DMs actuators patterns and the LGS WFSs sub-apertures.

The AOM finally delivers a corrected 30" FoV to the scientific instruments. The expected total WFE, including also NCPA, manufacturing and alignment tolerances, together with the AO correction term, evaluated through the simulations, corresponds to a SR larger than 10%, in bright end regime. The corrected beam is directed to one of the two scientific channels, Imager and Spectrograph, through a three-port selector. The third port is reserved for a visitor instrument.

The Imager uses a 4k×4k detector. The detector dewar can translate and rotate in tip-and tilt for alignment purposes through three independent linear stages. Two filter wheels are incorporated into the Imager.

The Spectrograph is composed of two spectrographs using an optical relay which spatially split the input field into two. Each spectrograph is dual arm and dual band, containing a dichroic beam splitter which separates
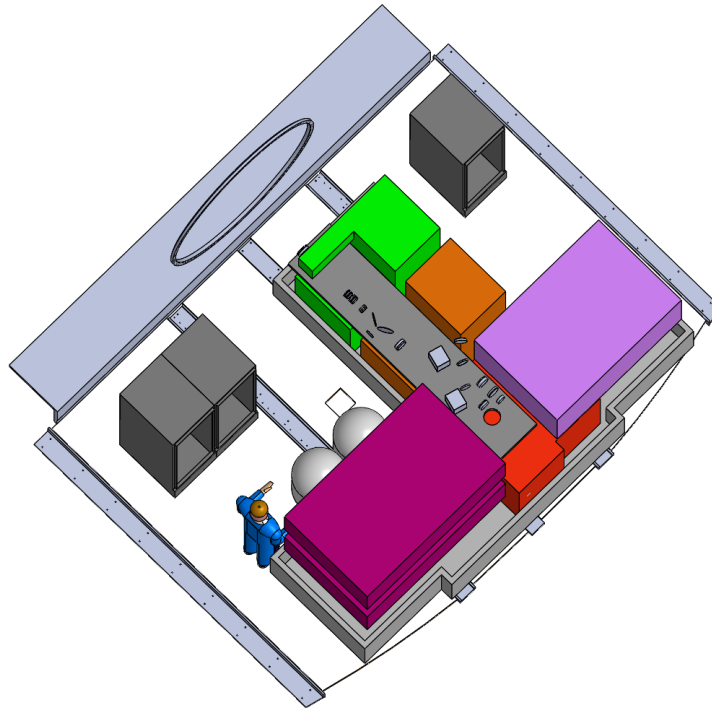
Figure 7. Current snapshot of the overall MAVIS mechanical layout on the AOF Nasmyth platform. The AOM PFR is the gray long optical table in the middle, surrounded by the LGS WFS space (orange), the Calibration unit (green), the NGS WFS (red), the imager (violet, right) and the spectrograph (purple, left). Cabinets are in dark grey. The interface to the AOF adaptor rotator is toward the top left.
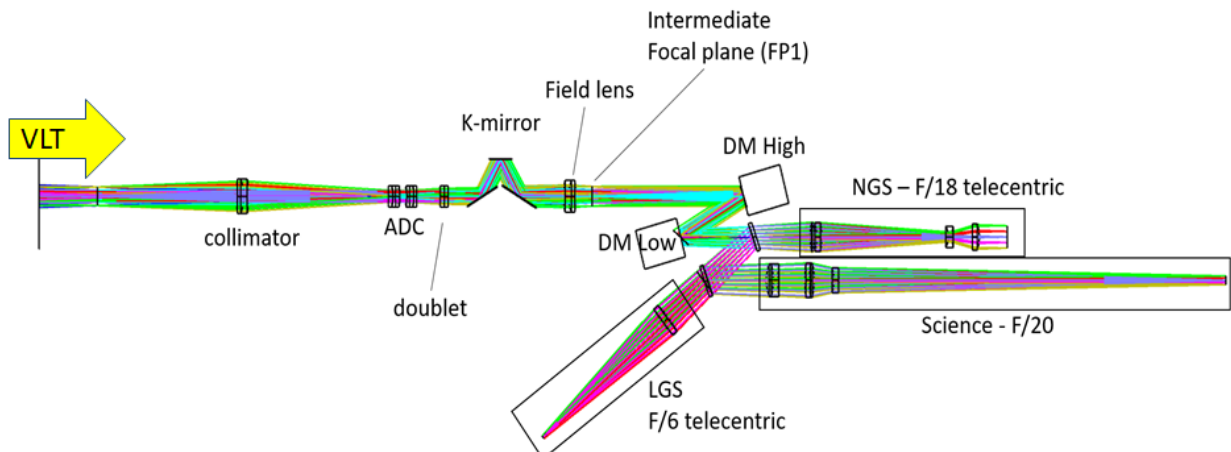

Figure 8. Optical layout of the MAVIS baseline transmissive PFR design. All powered optics are on-axis. Note that this optical layout will be reworked soon, e.g. the exact F/ ratios for NGS and LGS channels will be optimised.

the incoming light into two beams at different wavelengths. Moreover, each arm can operate at two different spectral resolution by changing the disperser element.

In addition to the MAVIS breakdown given above, the provision of the additional Guide Star Lasers (GSLs), which are necessary to achieve the instrument AO performance requirements, are currently considered to be within the MAVIS scope, in liaison with ESO.
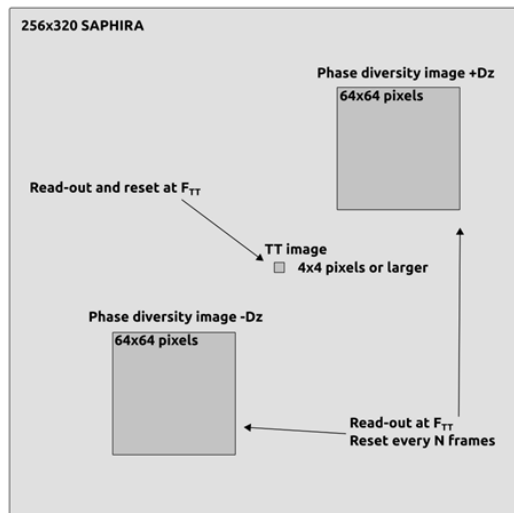
Figure 9. Conceptual layout of the NGS WFS chip occupation, including TT star image, together with phase diversity defocused image for truth sensing.

5. THE PATH TO FIRST LIGHT AND BEYOND

The MAVIS Phase A study has delivered a novel conceptual instrument design which satisfies the Top Level Requirements. The following project phases will develop further details by way of synthesising a complete Preliminary Design and the MAVIS Final Design, prior to the project moving into the manufacture, integration, verification and then commissioning phases.

The AIT concept for MAVIS is that all modules and sub-modules will be assembled and tested insofar as possible at the facilities of the individual institutes responsible for the development of those elements. Functional and performance verification will be performed before shipment for the global instrument integration and testing at AAO-Stromlo in Canberra, Australia.

MAVIS is having a very good start. A very strong consortium, with all the required expertise, has been put together. Eight months into the phase A, we have converged on a baseline design that verifies the ESO call for proposal TLRs. This baseline design includes an MCAO system with three DMs, 8 LGS WFSs, 3 NGS WFSs, and an imager covering 30"×30" at 7mas sampling and a monolithic IFU covering 3 to 6", with dual spectral resolution modes (5 and 10k). The phase A mid term review was passed successfully on October 2019. The phase A ends in May 2020. Assuming the instrument goes ahead into further phases, it should see starlight by the end of 2026 according to the current schedule.

MAVIS is shaping up to be a truely amazing facility, providing 3× the HST angular resolution and better sensitivity on point sources. MAVIS will be a workhorse facility instrument for the VLT into the 2030s, complementing very effectively facilities like the ELTs, and facing little competition in the current astronomical instrumentation landscape.

REFERENCES

[1] Finger, G., Baker, I., Alvarez, D., Ives, D., Mehrgan, L., Meyer, M., Stegmeier, J., and Weller, H. J., "Saphira detector for infrared wavefront sensing," in [*Adaptive Optics Systems IV*], **9148**, 914817, International Society for Optics and Photonics (2014).

[2] Agapito, G., Puglisi, A., and Esposito, S., "Passata: object oriented numerical simulation software for adaptive optics," in [*Adaptive Optics Systems V*], **9909**, 99097E, International Society for Optics and Photonics (2016).

[3] Nicolle, M., Fusco, T., Rousset, G., and Michau, V., "Improvement of shack–hartmann wave-front sensor measurement for extreme adaptive optics," *Optics letters* **29**(23), 2743–2745 (2004).